Journal of Visualized Experiments

Monitoring protein aggregation kinetics in vivo using automated inclusion counting in Caenorhabditis elegans

--Manuscript Draft--

Article Type:	Invited Methods Collection - JoVE Produced Video
Manuscript Number:	JoVE63365R2
Full Title:	Monitoring protein aggregation kinetics in vivo using automated inclusion counting in Caenorhabditis elegans
Corresponding Author:	Tessa Sinnige Utrecht University: Universiteit Utrecht Utrecht, Utrecht NETHERLANDS
Corresponding Author's Institution:	Utrecht University: Universiteit Utrecht
Corresponding Author E-Mail:	t.sinnige1@uu.nl
Order of Authors:	Jelle Molenkamp
	Anna den Outer
	Vera van Schijndel
	Tessa Sinnige
Additional Information:	
Question	**Response**
Please specify the section of the submitted manuscript.	Biochemistry
Please indicate whether this article will be Standard Access or Open Access.	Open Access ($3900)
Please indicate the **city, state/province, and country** where this article will be **filmed**. Please do not use abbreviations.	Utrecht, Utrecht, The Netherlands
Please confirm that you have read and agree to the terms and conditions of the author license agreement that applies below:	I agree to the Author License Agreement
Please confirm that you have read and agree to the terms and conditions of the video release that applies below:	I agree to the Video Release
Please provide any comments to the journal here.	

TITLE:

Monitoring Protein Aggregation Kinetics *In Vivo* Using Automated Inclusion Counting in *Caenorhabditis elegans*

AUTHORS AND AFFILIATIONS:

Jelle Molenkamp*, Anna den Outer*, Vera van Schijndel*, Tessa Sinnige

Bijvoet Centre for Biomolecular Research, Utrecht University, The Netherlands

Email addresses of co-authors:

Jelle Molenkamp (w.h.molenkamp@students.uu.nl)
Anna den Outer (a.j.denouter@students.uu.nl)
Vera van Schijndel (v.vanschijndel@students.uu.nl)

*Equal contribution

Corresponding author:

Tessa Sinnige (t.sinnige1@uu.nl)

SUMMARY:

Here, a method is presented for the analysis of protein aggregation kinetics in the nematode *Caenorhabditis elegans*. Animals from an age-synchronized population are imaged at different time points, followed by semiautomated inclusion counting in CellProfiler and fitting to a mathematical model in AmyloFit.

ABSTRACT:

Protein aggregation into insoluble inclusions is a hallmark of a variety of human diseases, many of which are age-related. The nematode *Caenorhabditis elegans* is a well-established model organism that has been widely used in the field to study protein aggregation and toxicity. Its optical transparency enables the direct visualization of protein aggregation by fluorescence microscopy. Moreover, the fast reproductive cycle and short lifespan make the nematode a suitable model to screen for genes and molecules that modulate this process.

However, the quantification of aggregate load in living animals is poorly standardized, typically performed by manual inclusion counting under a fluorescence dissection microscope at a single time point. This approach can result in high variability between observers and limits the understanding of the aggregation process. In contrast, amyloid-like protein aggregation *in vitro* is routinely monitored by thioflavin T fluorescence in a highly quantitative and time-resolved fashion.

Here, an analogous method is presented for the unbiased analysis of aggregation kinetics in living *C. elegans*, using a high-throughput confocal microscope combined with custom-made image analysis and data fitting. The applicability of this method is demonstrated by monitoring inclusion formation of a fluorescently labeled polyglutamine (polyQ) protein in the body wall muscle cells.

The image analysis workflow allows the determination of the number of inclusions per animal, which are fitted to a mathematical model based on independent nucleation events in individual muscle cells. The method described here may prove useful to assess the effects of proteostasis factors and potential therapeutics for protein aggregation diseases in a living animal in a robust and quantitative manner.

INTRODUCTION:

The accumulation of misfolded proteins into insoluble deposits occurs in a wide range of diseases. Well-known examples are the aggregation of amyloid-β and tau in Alzheimer's disease, α-synuclein in Parkinson's disease, and huntingtin with expanded polyQ in Huntington's disease[1,2]. The misfolding of these polypeptides into amyloid fibrils is associated with toxicity and cell death by mechanisms that are still largely unclear. Elucidating the mechanisms of amyloid formation will be crucial to developing effective therapies that are currently unavailable.

Detailed investigations of amyloid formation have been performed *in vitro* based on thioflavin T fluorescence measurements, leading to a mechanistic understanding of the aggregation process and the effect of inhibitory molecules[3–5]. However, it is not clear whether the same aggregation mechanisms hold true in the complex environment of living cells and organisms. The nematode worm *Caenorhabditis elegans* is a suitable model organism to study protein aggregation *in vivo*. It has a relatively simple anatomy but consists of multiple tissues, including muscle, intestine, and a nervous system. It is genetically well-characterized, and tools for genetic modification are readily available. Furthermore, it has a short generation time of ~3 days and a total lifespan of 2–3 weeks. As such, protein aggregation can be examined across the lifespan of the animal on an experimentally convenient timescale. Finally, the nematode is optically transparent, enabling the tracking of the aggregation of fluorescently labeled proteins in live animals.

These features of *C. elegans* have been previously exploited to investigate the aggregation of polyQ proteins as a model for Huntington's and other polyQ expansion diseases. Above the pathogenic threshold of 35–40 glutamine residues, the polyQ proteins labeled with yellow fluorescent protein (YFP) can be observed to form insoluble inclusions in the muscle tissue[6,7], neurons[8], and the intestine[9,10]. These features have been widely used to screen for genes[11–13] and small-molecule modifiers[14] of protein aggregation and toxicity.

C. elegans has the potential to play an important role in bridging the gap between *in vitro* studies of protein aggregation and more complex disease models such as mice[15]. *C. elegans* is amenable to drug screening[16] but can also be exploited to obtain a fundamental understanding of the molecular mechanisms of protein aggregation *in vivo*, as demonstrated recently[17]. However, for both applications, it is of prime importance to extract a quantitative and reproducible measure of protein aggregation. Here, this is achieved with the use of a high-throughput confocal microscope combined with a dedicated image analysis pipeline (**Figure 1**).

PROTOCOL:

1. Growth of an age-synchronized population of *C. elegans*

1.1. Maintain the *C. elegans* strains on nematode growth medium (NGM) plates seeded with *Escherichia coli* OP50 at 20 °C according to standard procedures[18].

1.2. Perform a synchronized egg-lay by placing 10 adult nematodes onto a 6 cm seeded NGM plate with a platinum worm pick. Leave the adults to lay eggs for ~2 h at 20 °C before removing them. Pick 1–4 plates per strain, depending on the fertility of the strain and the number of time points to be taken.

1.3. Place the plates with eggs in the incubator at 20 °C. Monitor the development of the animals until they reach adulthood.

NOTE: The day on which the animals have reached adulthood is defined here as day 1. Typically, this is three days after the egg-lay.

1.4. Starting from day 1, transfer the animals to freshly seeded NGM plates daily to separate them from their offspring. To compensate for animals that die or are lost during transfer, transfer ~40 animals per strain times the number of points to be imaged (see step 2). Proceed until the animals have ceased to lay fertilized eggs (~day 6 of adulthood).

NOTE: Exclude animals with bagging or other developmental phenotypes. Bagging is commonly observed in strains expressing aggregation-prone proteins.

2. Sample preparation of *C. elegans* in a multiwell plate

NOTE: As the imaging procedure requires anesthetics that will eventually kill the animals, the same animals cannot be reused for subsequent time points. Instead, different animals from the same age-synchronized batch are imaged on different days. Even though most strains will have few inclusions at day 1, it is recommended to include this time point as a baseline.

2.1. Prepare the 384-well plate by filling the required number of wells with 100 µL of M9 buffer supplemented with 25 mM NaN_3 as an anesthetic. Fill one well per strain to be imaged.

NOTE: Sodium azide (NaN_3) is toxic and should be handled with care.

2.2. For each strain, transfer 20 animals into one well using a platinum worm pick.

NOTE: The worms must be placed outside the bacterial lawn before placing them in the well. Bacteria make the animals adhere to the worm pick, which can prevent their release and will cloud the well contents. Generally, 20 is the optimal number of animals per well to prevent overlap between the worms while limiting unnecessary imaging of empty well space.

2.3. Cover the plate with the lid to prevent evaporation, and image the plate within 1 h after preparation.

2.4. Repeat steps 2.1–2.3 daily until a steady plateau in the inclusion numbers is reached or until most animals have died. Perform the sample preparation and imaging at the same time every day to ensure intervals of 24 h.

3. Image acquisition on the high-throughput confocal microscope

NOTE: This experiment can also be set up on a regular spinning disk confocal microscope with a multiwell plate holder. A camera with a large field-of-view is beneficial to limit the number of tiles needed to be imaged to span the entire well. See the **Table of Materials** for details about the microscope and software used in this protocol.

3.1. Switch on the instrument and open the software.

3.2. Start a new protocol by going to **Measurement Settings** | **New**. Select the correct multiwell plate type and click **Create a New Measurement Setting**.

3.3. Set up the channel for fluorescence by going to **Ch 1**. Set the objective to **10x**. Select **488 nm** as the light source and **BP525/25** as the emission filter to image YFP. Set binning to **2x2** to reduce file size.

3.4. Click **Add Channel** and select **Brightfield** as the method.

3.5. To add a z-stack confocal fluorescence image to the measurement, choose **3D Fluorescence acquisition** under **Action List**. Go to **Select** and choose **Ch 1**. To minimize file sizes, set **Image Processing** to **Maximum** so that the maximum projection image is saved rather than the full z-stack.

3.6. Click **BF/Ph Acquisition | Select | Ch 2** for the brightfield channel.

3.7. Click on the **play** button (look for the right-pointing triangle symbol) next to **Unload Well Plates** and place the 384-well plate in the microscope.

3.8. Under **3D Fluorescence Acquisition**, click **Test** and select a well containing worms to determine the optimal shifting distance at which the worms are centered correctly. Set **Ascending Distance** to 50 µm, **Descending Distance** to -50 µm, and **Slicing Interval** to 2 µm to capture the entire thickness of the animals in the z-stack.

3.9. Optimize the exposure time to get a good signal intensity for all four strains while avoiding saturation. Use the same exposure time for all strains and time points.

3.10. Select the wells to be imaged under **Well Plate Scan Setting**. Select **Tile** and **Acquire Whole Well**.

3.11. Save the **Measurement Setting** and start the experiment by clicking **Start Measurement**. For subsequent time points, open the same Measurement Setting and adjust the shifting distance and the wells to be imaged.

4. Stitching tiled images in ImageJ

NOTE: This step is only required when using an objective larger than 4x, for which the image of each well is acquired as multiple tiles. In this analysis workflow, stitching of the tiles is performed using the free software FIJI/ImageJ[19] (**Figure 2**). Depending on the instrument used in step 3, it may also be possible to perform stitching directly in the accompanying software.

4.1. Download FIJI[20] and open it.

4.2. Go to **Plugins | Stitching | Grid/Collection Stitching**[21].

4.3. In the popup window, **Grid/Collection Stitching**, select the **type** and **order** by which the tiles were collected. Choose **grid: row-by-row** and **right & down**.

4.4. In the next window, **Grid stitching: Grid: row-by-row, Right & Down**, insert the number of tiles in x and y directions. For the 10x objective used here, choose **2** as the **grid size x**, **3** as the **grid size y**, and **0** as the **tile overlap**.

4.5. Click **browse** and select the folder containing the images to be stitched in tiff format.

4.6. Insert the common file name under **File names for tiles**, using **{i}** at the position of the tile number in each file name.

4.7. Untick all boxes below.

4.8. Run the plugin.

4.9. Save the resulting images as tiff files for analysis in the next step.

5. Automated inclusion counting using CellProfiler[22]

5.1. Download and install the open-source image analysis software, CellProfiler[23]. Download the **InclusionCounting.cpproj** pipeline from **github.com/sinnigelab/aggregate-quantification**.

5.2. Open CellProfiler and drag the pipeline into the **Drop a pipeline file here** window. Click **Yes** to load the project.

5.3. Click on the **Images** input module and drag the stitched images into the window **Drop files and folder here**.

5.4. Click on the **Metadata** input module. Adjust **Regular expression to extract from file name** according to the names of the stitched images.

5.5. Click on the **NamesandTypes** input module and adjust **Select the rule criteria** to match the channels in the file names.

NOTE: In the default settings of the pipeline, file names containing **BF** are recognized as brightfield images and are named **Worms**. File names containing **YFP** are recognized as fluorescence images and are named **Fluorescence**.

5.6. Click on **View output settings** to select a default folder to save the output from CellProfiler.

5.7. Click on **Start Test Mode** to check the settings of the pipeline using the first imaging dataset. Click on **Run** to run through all modules in the pipeline or **Step** to run through the pipeline one module at a time. To adjust the worm outlines in the **EditObjectsManually** module, click on **help** to see the instructions and click on **Done** to continue running the pipeline.

NOTE: The extracted measurements will not be exported while in **Test** mode. The typical pixel sizes for worms and inclusions may need to be adjusted based on the strains and magnification used.

5.8. Click on **Exit Test Mode** and **Analyze Images**.

5.9. Open the output folder to view the output files. Open the images with the original file name followed by **outlines** to check whether the worms and inclusions were correctly overlaid.

NOTE: The number of inclusions per worm can be found in the file named **ExpandedWormObjects**. More information about the input images can be found in the file named **Image**. Additional output can be selected in the **ExportToSpreadsheet** module in the pipeline.

6. Global fitting of inclusion count data using AmyloFit[5]

NOTE: This step can only be performed when data for multiple protein concentrations are available. For Q40-YFP, a set of four strains with different levels of overexpression in the body wall muscle cells has been created previously[17]. In other cases, novel strains should be generated using plasmid microinjection and genomic integration[24].

6.1. Go to the free online fitting platform for aggregation kinetics AmyloFit[25]. Either register or log in with an existing account.

NOTE: An extensive manual on how to use AmyloFit can be accessed for additional help. See the link on the top-left of the webpage (after login) for more information.

6.2. To start using AmyloFit, **name** the project and click on **Create project.** Open the project by clicking on **Open** and create a session by giving it a name and clicking on **Create & load session**.

6.3. Click **Add Data** and upload the file containing the average numbers of inclusions per animal, following the data format requirements shown in the left panel. Click **Load New Data**.

6.4. Skip the preprocessing steps, which are not required for inclusion count data, by setting **number of points to average over for zero-point offset** and **number of points to average over for plateau** to **0**. Click **Submit**. Repeat this step for each protein concentration (i.e., each column in the uploaded file).

6.5. Select **Custom** in the model panel, enter **Ncells*(1-exp(-Kcell*m**(n)*(t-1)))** in the equation box and click **Load model**.

NOTE: As AmyloFit was originally designed for the analysis of kinetic data from *in vitro* assays, a custom-made model must be loaded to analyze the inclusion count data of *C. elegans.* In the equation used here, N_{cells} is the number of cells in which inclusion formation takes place, K_{cell} is the nucleation rate constant, m the intracellular protein concentration, and n the reaction order of nucleation.

6.6. Set the parameter types to **Global Const** for N_{cells}, **Global fit** for K_{cell} and n, and **Const** for m. Set **Value** of N_{cells} to **95** for body wall muscle cells and **Initial guess** for K_{cell} and n to **1**. Enter the values of m for the different strains in the left panel.

NOTE: Initial guesses are not relevant for the relatively simple model used here. For more complex models, it is beneficial to enter an estimate of the expected values to shorten the calculation time.

6.7. Leave the number of basin hops unchanged and click **Fit** in the fitting panel.

6.8. Extract the fit by clicking **Download Data and Fit.**

NOTE: The parameters extracted by the global fit of the model will be listed in the bottom-right corner. A plot of the data and fit will be automatically generated in the top-right panel. This plot can be extracted by clicking **Download pdf** and customized by going to **Display Plot Options**. K_{cell} has units of concentration^{-n+1}time^{-1}. To compare values with different n, K_{cell} can be converted to the nucleation rate at a given protein concentration by multiplying it with m^n.

REPRESENTATIVE RESULTS:

The method described here (**Figure 1**) was used to analyze the aggregation kinetics of a construct comprising 40 glutamines fused to YFP (Q40-YFP). The protein is expressed under the control of the unc-54 promoter, driving expression in the body wall muscle cells. As these are relatively large and easy to visualize, the use of a 10x objective is sufficient to resolve the individual

inclusions formed by Q40-YFP. Four strains (lines A–D) were previously developed expressing the protein to different extents to assess the concentration-dependence of polyQ aggregation *in vivo*[17].

Age-synchronized populations of lines A–D were generated by a 2 h egg-lay, followed by daily transfer once the offspring reached adulthood. From day 1 to day 10 of adulthood, 20 animals from each of the four strains were imaged in a 384-well plate, using a high-throughput confocal microscope. The images of the wells were acquired as 6 tiles, which were stitched together using a plugin in ImageJ[21] (**Figure 2**). The stitched images were subsequently analyzed using a custom-made CellProfiler[22] pipeline (**Figure 3**) to quantify the average inclusion number per animal for each strain and time point.

The data were then fitted to a mathematical model in AmyloFit[5] (**Figure 4**). The model is based on the assumption that each of the 95 body wall muscle cells independently acquires one inclusion by a rate-limiting nucleation event, followed by fast aggregate growth[17]. The fit yielded a nucleation rate constant of 1.9×10^{-11} $M^{-1.1}$ s^{-1} and a reaction order of 2.1, corresponding to a nucleation rate of 0.016 molecules h^{-1} per cell at an intracellular protein concentration of 1 mM. Two independent biological replicates led to closely corresponding values for the nucleation rate and reaction order, which are in agreement with a previous study using a similar protocol[17] (**Table 1**).

FIGURE AND TABLE LEGENDS:

Figure 1: Schematic overview of the method. (**A**) Age-synchronized *C. elegans* populations are generated by a timed egg-lay. (**B**) Animals from the same population are imaged in a 384-well plate at different time points. (**C**) The tiles are stitched together to form images of the entire wells, which are analyzed in CellProfiler to quantify the inclusion numbers per animal. (**D**) The data are fitted to a mathematical model using AmyloFit.

Figure 2: Screenshots of the stitching procedure in ImageJ using the plugin Grid/Collection stitching[21].

Figure 3: Schematic of the CellProfiler pipeline to quantify inclusions numbers. (**A–C**) The brightfield image (**A**) is used to identify the worms (**B**, close-up in **C**). (**D–G**) The fluorescence image (**D**, close-up in **E**) is used to identify the inclusions (**F**). The worms and inclusions are related to provide the number of inclusions for each worm in the well (**G**). The images shown are of Q40 line A animals at day 3 of adulthood.

Figure 4: Fitting the data to a mathematical model in AmyloFit. (**A**) Data are uploaded to AmyloFit. (**B**) A custom equation is entered to model inclusion formation, assuming independent nucleation events in each cell. (**C**) Fitting of the aggregation kinetics for *C. elegans* lines A–D expressing different levels of Q40-YFP. The data are representative of two independent biological replicates.

Table 1: Values of the nucleation rate and reaction order of Q40-YFP aggregation. Data for two

independent biological replicates of the protocol and comparison with previously published data[17].

DISCUSSION:

The method presented herein facilitates an unbiased and quantitative analysis of protein aggregation kinetics in the model organism *C. elegans*. It depends on four key elements (**Figure 1**): 1) maintaining an age-synchronized population of nematodes; 2) fluorescence microscopy in multiwell plates; 3) automated inclusion counting in CellProfiler; 4) data fitting in AmyloFit. Compared to manual counting of inclusions in freely moving animals or from saved images[26], quantification in CellProfiler is both faster and more unbiased. The other key advancement of the protocol is the acquisition of kinetic data, rather than single timepoints, which provides quantitative insights into the aggregation mechanism upon fitting the data to a mathematical model.

The four elements of the protocol can be used as independent modules that can be modified depending on the application. Age-synchronized populations can also be maintained using 5-fluoro-2'-deoxyuridine (FUDR) to sterilize the animals. This compound affects lifespan and proteostasis[24,25] and is highly carcinogenic to the experimenter; however, it precludes manual transfer of the worms, which can be labor-intensive when large numbers are handled. Other alternatives are the use of sterile mutants[29] or filtration devices to separate offspring[30].

The fluorescence microscopy step can also be adjusted, for example, using higher magnifications to monitor protein aggregation in neurons. Widefield microscopy may be sufficient to monitor polyQ aggregation in muscle cells when the relative difference between conditions is more important than the absolute numbers of inclusions. The CellProfiler pipeline can still be used in these cases, although the settings (pixel size and intensity threshold to recognize worms and inclusions) will need to be adjusted by the user. The throughput of the technique is currently limited by the need for manual picking of the animals into the 384-well plate. This can potentially be remedied by the use of microfluidic devices[16]. Sodium azide is a relatively harsh anesthetic, which could be replaced by physical immobilization with hydrogels or beads[28,29].

The analysis in AmyloFit presented here is based on an aggregation mechanism consisting of independent nucleation events in individual cells. In cases where this model does not fit, the user should consider an alternative such as the cooperative aggregation model developed previously[17]. A limitation of this approach is that strains expressing the protein of interest at different concentrations need to be available, although these can be generated using routine *C. elegans* methods[24].

Altogether, this protocol provides the means to obtain high-quality data for protein aggregation kinetics in an *in vivo* model system, allowing for detailed analysis of aggregation mechanisms[17]. Although the method was demonstrated for polyQ aggregation in the *C. elegans* muscle tissue, future applications of the protocol may include other proteins and tissues and study the effects of proteostasis factors and small molecules.

ACKNOWLEDGMENTS:

We thank the Morimoto lab for *C. elegans* strains and Esmeralda Bosman for assistance on the high-throughput confocal microscope. This work was funded by a start-up grant from Utrecht University to T.S.

DISCLOSURES:

The authors have no conflicts of interest to disclose.

REFERENCES:

1. Knowles, T. P. J., Vendruscolo, M., Dobson, C. M. The amyloid state and its association with protein misfolding diseases. *Nature Reviews. Molecular Cell Biology*. **15** (6), 384–396 (2014).
2. Chiti, F., Dobson, C. M. Protein misfolding, amyloid formation, and human disease: a summary of progress over the last decade. *Annual Review of Biochemistry*. **86** (1), 27–68 (2017).
3. Knowles, T. P. J. et al. An analytical solution to the kinetics of breakable filament assembly. *Science*. **326** (5959), 1533–1537 (2009).
4. Cohen, S. I. A. et al. Proliferation of amyloid-β42 aggregates occurs through a secondary nucleation mechanism. *Proceedings of the National Academy of Sciences of the United States of America*. **110** (24), 9758–9763 (2013).
5. Meisl, G. et al. Molecular mechanisms of protein aggregation from global fitting of kinetic models. *Nature Protocols*. **11** (2), 252–272 (2016).
6. Satyal, S. H. et al. Polyglutamine aggregates alter protein folding homeostasis in *Caenorhabditis elegans*. *Proceedings of the National Academy of Sciences of the United States of America*. **97** (11), 5750–5755 (2000).
7. Morley, J. F., Brignull, H. R., Weyers, J. J., Morimoto, R. I. The threshold for polyglutamine-expansion protein aggregation and cellular toxicity is dynamic and influenced by aging in *Caenorhabditis elegans*. *Proceedings of the National Academy of Sciences of the United States of America*. **99** (16), 10417–10422 (2002).
8. Brignull, H. R., Moore, F. E., Tang, S. J., Morimoto, R. I. Polyglutamine proteins at the pathogenic threshold display neuron-specific aggregation in a pan-neuronal *Caenorhabditis elegans* model. *Journal of Neuroscience*. **26** (29), 7597–7606 (2006).
9. Moronetti Mazzeo, L. E., Dersh, D., Boccitto, M., Kalb, R. G., Lamitina, T. Stress and aging induce distinct polyQ protein aggregation states. *Proceedings of the National Academy of Sciences of the United States of America*. **109** (26), 10587–10592 (2012).
10. Prahlad, V., Morimoto, R. I. Neuronal circuitry regulates the response of *Caenorhabditis elegans* to misfolded proteins. *Proceedings of the National Academy of Sciences of the United States of America*. **108** (34), 14204–14209 (2011).
11. Nollen, E. A. A. et al. Genome-wide RNA interference screen identifies previously undescribed regulators of polyglutamine aggregation. *Proceedings of the National Academy of Sciences of the United States of America*. **101** (17), 6403–6408 (2004).
12. Silva, M. C. et al. A genetic screening strategy identifies novel regulators of the proteostasis network. *PLoS Genetics*. **7** (12), e1002438 (2011).
13. Brehme, M. et al. A chaperome subnetwork safeguards proteostasis in aging and neurodegenerative disease. *Cell Reports*. **9**, 1–16 (2014).
14. Calamini, B. et al. Small-molecule proteostasis regulators for protein conformational

diseases. *Nature Chemical Biology*. **8** (2), 185–196 (2012).
15. Sinnige, T., Stroobants, K., Dobson, C. M., Vendruscolo, M. Biophysical studies of protein misfolding and aggregation in *in vivo* models of Alzheimer's and Parkinson's diseases. *Quarterly Reviews of Biophysics*. **49**, e22 (2020).
16. Mondal, S. et al. Large-scale microfluidics providing high-resolution and high-throughput screening of *Caenorhabditis elegans* poly-glutamine aggregation model. *Nature Communications*. **7** (1), 13023 (2016).
17. Sinnige, T. et al. Kinetic analysis reveals that independent nucleation events determine the progression of polyglutamine aggregation in *C. elegans*. *Proceedings of the National Academy of Sciences of the United States of America*. **118** (11), e2021888118 (2021).
18. Brenner, S. *Caenorhabditis elegans*. *Methods*. **77** (1), 71–94 (1974).
19. Schindelin, J. et al. Fiji: an open-source platform for biological-image analysis. *Nature Methods*. **9** (7), 676–682 (2012).
20. FIJI/ImageJ. https://imagej.net/downloads (2021).
21. Preibisch, S., Saalfeld, S., Tomancak, P. Globally optimal stitching of tiled 3D microscopic image acquisitions. *Bioinformatics*. **25** (11), 1463–1465 (2009).
22. Lamprecht, M. R., Sabatini, D. M., Carpenter, A. E. CellProfiler: free, versatile software for automated biological image analysis. *BioTechniques*. **42** (1), 71–75 (2007).
23. Broad Institute. CellProfiler. https://cellprofiler.org/releases (2021).
24. Mello, C. C., Kramer, J. M., Stinchcomb, D., Ambros, V. Efficient gene transfer in *C. elegans*: extrachromosomal maintenance and integration of transforming sequences. *EMBO Journal*. **10** (12), 3959–3970 (1991).
25. Knowles group, University of Cambridge. Amylofit. https://amylofit.com/amylofitmain/login/ (2021).
26. Lazaro-Pena, M. I., Cornwell, A. B., Samuelson, A. V. Quantifying tissue-specific proteostatic decline in *Caenorhabditis elegans*. *Journal of Visualized Experiments: JoVE*. (175), doi: 10.3791/61100 (2021).
27. Feldman, N., Kosolapov, L., Ben-Zvi, A. Fluorodeoxyuridine improves *Caenorhabditis elegans* proteostasis independent of reproduction onset. *PLoS One*. **9** (1), e85964 (2014).
28. Brunquell, J., Bowers, P., Westerheide, S. D. Fluorodeoxyuridine enhances the heat shock response and decreases polyglutamine aggregation in an HSF-1-dependent manner in *Caenorhabditis elegans*. *Mechanisms of Ageing and Development*. **141–142**, 1–4 (2014).
29. David, D. C. et al. Widespread protein aggregation as an inherent part of aging in *C. elegans*. *PLoS Biology*. **8** (8), 47–48 (2010).
30. Hunter, S., Maulik, M., Scerbak, C., Vayndorf, E., Taylor, B. E. Caenorhabditis sieve: A low-tech instrument and methodology for sorting small multicellular organisms. *Journal of Visualized Experiments: JoVE*. (137), 1–12, doi: 10.3791/58014 (2018).
31. Burnett, K., Edsinger, E., Albrecht, D. R. Rapid and gentle hydrogel encapsulation of living organisms enables long-term microscopy over multiple hours. *Communications Biology*. **1**, 73 (2018).
32. Dong, L. et al. Reversible and long-term immobilization in a hydrogel-microbead matrix for high-resolution imaging of *Caenorhabditis elegans* and other small organisms. *PLoS One*. **13** (3), e0193989 (2018).

Figure 1

Click here to access/download;Figure;Jove

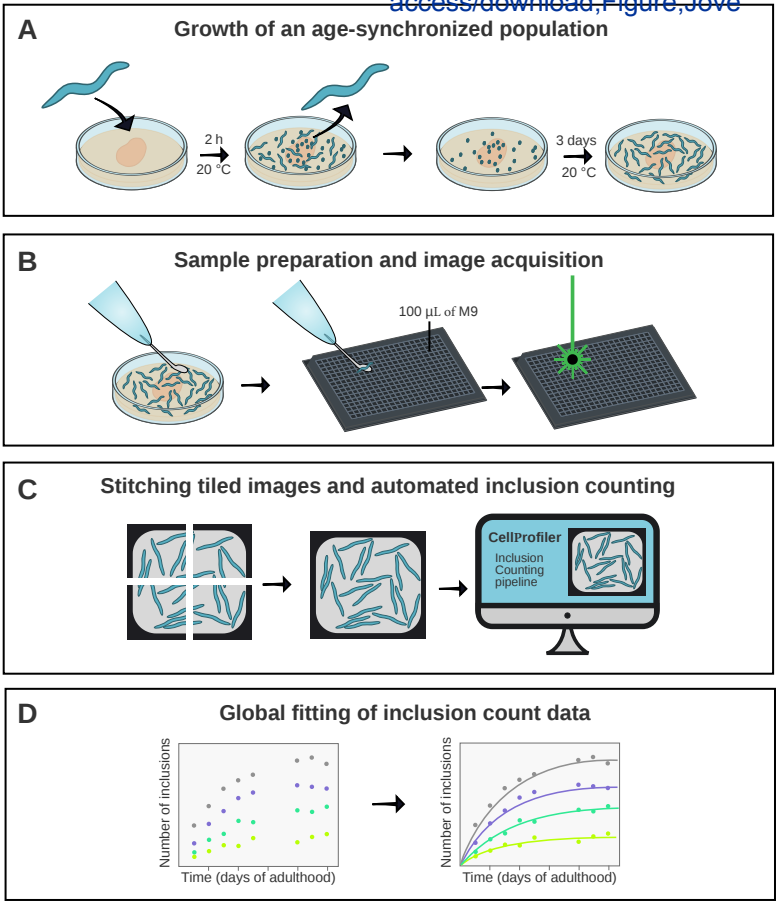

Figure 2

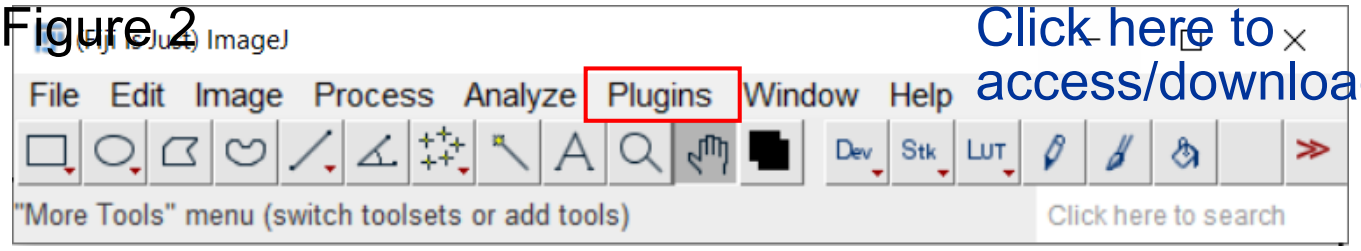

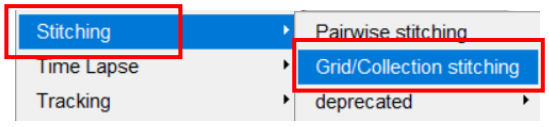

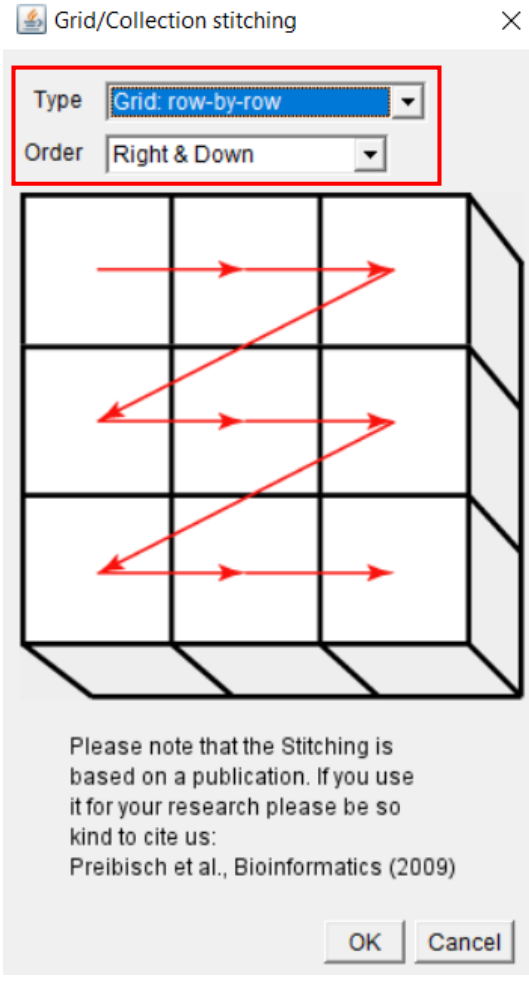

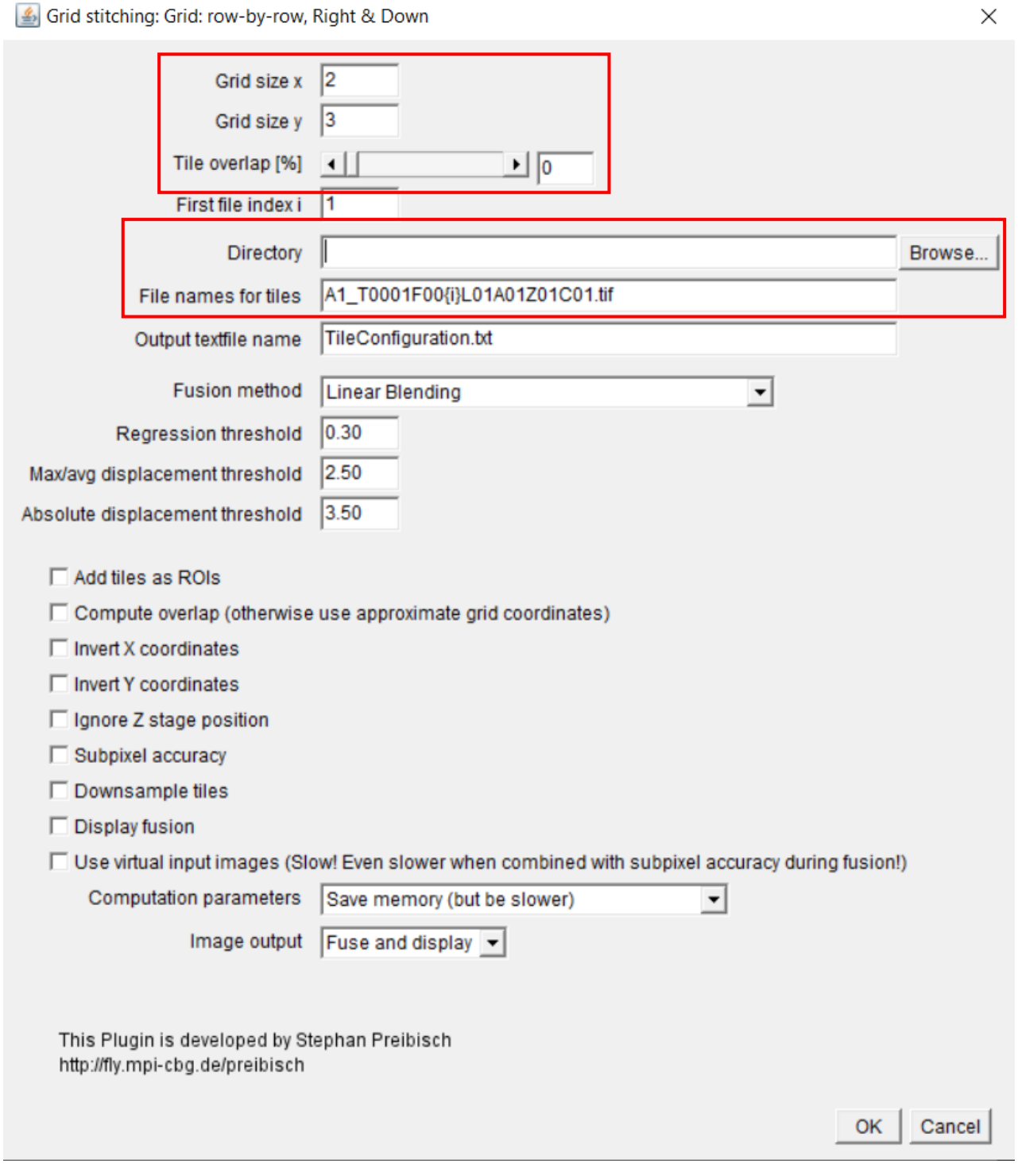

Figure 3

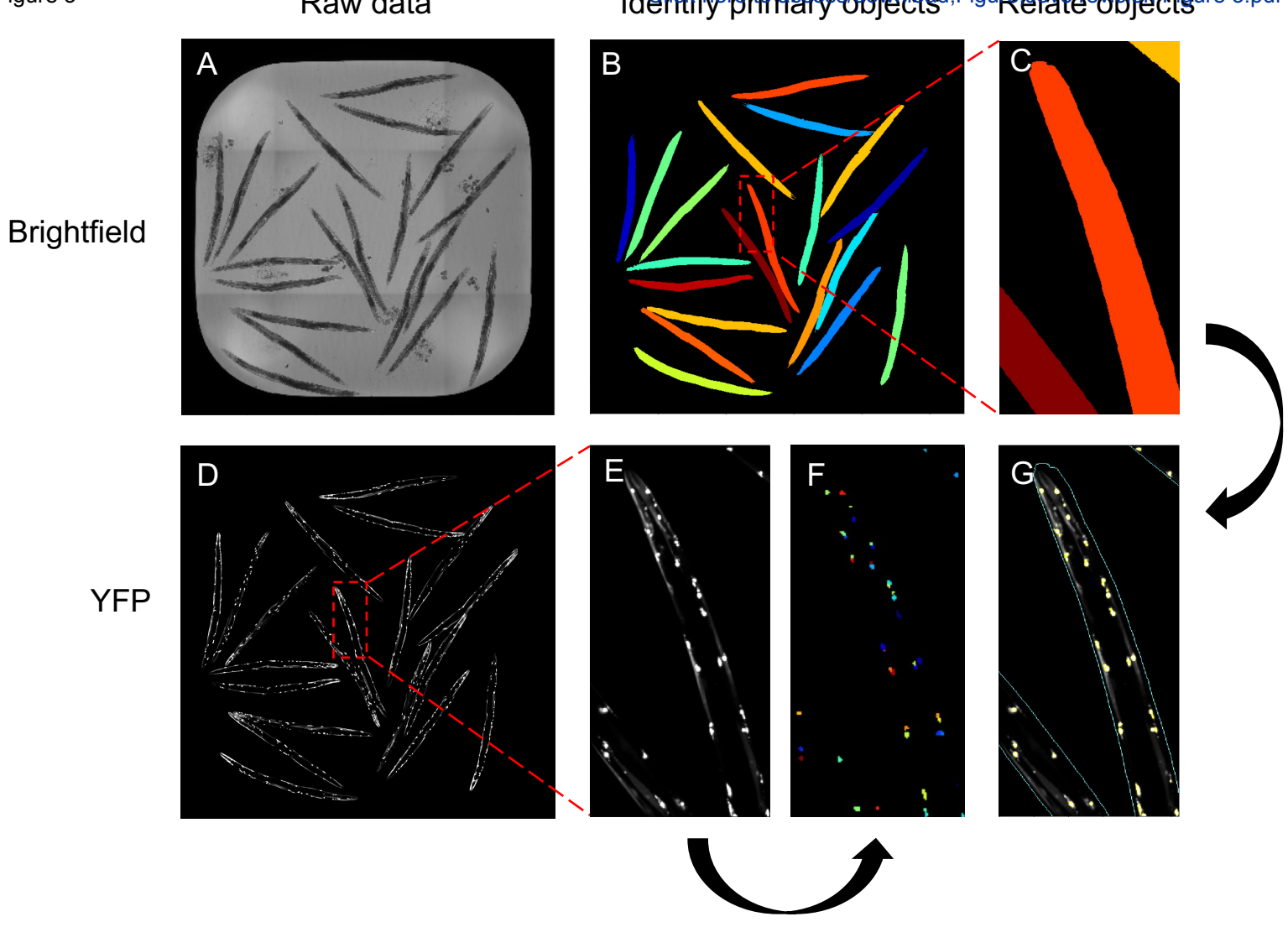

Figure 4

A

Upload data

AmyloFit

Time	Line A	Line B	Line C	Line D
1	....	....	....	....
2	....	....	....	....
3	....	....	....	....
....	....	....	....	....
10	....	....	....	....

B

Load model

Model

Half Time Plotter

Select fit type and initial guess for each parameter.

Custom

Load model

Equation :

Ncells*(1-exp(-Kcell*m**(n)*(t-1)))

$N_{cells} \cdot (1 - \exp(-K_{cell} \cdot m^n \cdot (t-1)))$

Select parameter type below:

N_{cells} Fit Global fit Group fit Const Global Const
Value : 95
in units of unknown units

K_{cell} Fit Global fit Group fit Const Global Const
Initial guess : 1
in units of unknown units

m Fit Global fit Group fit Const Global Const
Input values in 'Data' section on the left
in units of unknown units

n Fit Global fit Group fit Const Global Const
Initial guess : 1
in units of unknown units

Save fitting parameters | Load saved fitting parameters

C

Fit data

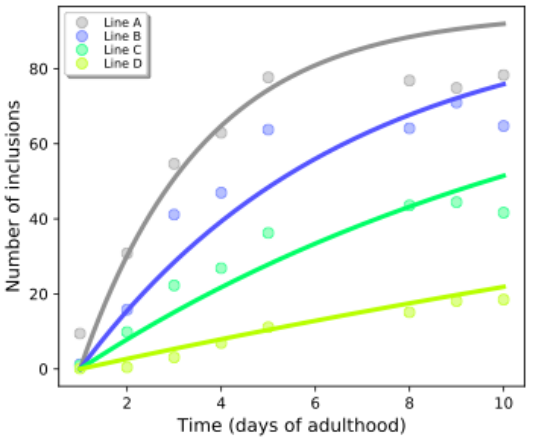

Table 1

	Dataset 1	Dataset 2	Sinnige et al.[17]
Reaction order	2.1	1.9	1.6
Nucleation rate constant at 1 mM ($M\ s^{-1}$)	7.3×10^{-18}	4.1×10^{-18}	6.7×10^{-18}
Molecules h^{-1} $cell^{-1}$ at 1 mM	0.016	0.009	0.015

Editorial comments:

1. Please take this opportunity to thoroughly proofread the manuscript to ensure that there are no spelling or grammar issues.

Ok.

2. Please revise the text to avoid the use of any personal pronouns (e.g., "we", "you", "our" etc.).

All personal pronouns have been removed.

3. JoVE cannot publish manuscripts containing commercial language. This includes trademark symbols (™), registered symbols (®), and company names before an instrument or reagent. Please remove all commercial language from your manuscript and use generic terms instead. All commercial products should be sufficiently referenced in the Table of Materials.
For example: Excel, CellProfiler,etc.

CellProfiler is open-source software. We have included this notion in step 5.1 and included the reference (line 217 in the revised manuscript). The sentence containing Excel has been removed in response to point 4 and reviewer 3 major point 5.

4. Please ensure that all text in the protocol section is written in the imperative tense as if telling someone how to do the technique (e.g., “Do this,” “Ensure that,” etc.). The actions should be described in the imperative tense in complete sentences wherever possible. Avoid usage of phrases such as “could be,” “should be,” and “would be” throughout the Protocol. Any text that cannot be written in the imperative tense may be added as a “Note.” However, notes should be concise and used sparingly. Please include all safety procedures and use of hoods, etc.

We have revised the protocol accordingly.

5. Please note that your protocol will be used to generate the script for the video and must contain everything that you would like shown in the video. Please add more details to your protocol steps. Please ensure you answer the “how” question, i.e., how is the step performed? Alternatively, add references to published material specifying how to perform the protocol action. Please add more specific details (e.g. button clicks for software actions, numerical values for settings, etc) to your protocol steps. There should be enough detail in each step to supplement the actions seen in the video so that viewers can easily replicate the protocol.

We have included all of the button clicks and settings in the revised version, in particular in steps 3 and 6.

6. Line 106-111: how is the sample prepared? What is the anesthetic used in this study?

This step (2.1) has been removed from the protocol, as it was a general comment referring to the steps below.

7. Line 113: Composition of M9 buffer? Does the M9 buffer only contain Sodium azide?

The composition of the M9 buffer is mentioned in the Materials Table. To avoid confusion, we have rewritten this to “M9 buffer supplemented with 25 mM NaN3” (Line 124 in the revised manuscript).

8. Line 149/192: Please add the link to the references and cite the appropriate reference number here.

We moved the links to the reference list.

9. Please include a one-line space between each protocol step and then highlight up to 3 pages of the Protocol (including headings and spacing) that identifies the essential steps of the protocol for the video, i.e., the steps that should be visualized to tell the most cohesive story of the Protocol. Remember that non-highlighted Protocol steps will remain in the manuscript, and therefore will still be available to the reader.

We have included the spacing and highlighted the steps for the video.

10. As we are a methods journal, please ensure that the Discussion explicitly covers the following in detail in 3-6 paragraphs with citations:
a) Critical steps within the protocol
b) Any modifications and troubleshooting of the technique
c) Any limitations of the technique
d) The significance with respect to existing methods
e) Any future applications of the technique

We rewrote the Discussion to cover these points more explicitly, at the same time addressing some of the reviewers' comments as detailed below.

11. Please ensure that all the supplies (chemicals, reagents, equipment, software, etc.) used in this study are included in the Table of Materials.

We have checked the Table carefully and made one adjustment according to reviewer 3, major point 1 ("confocal microscope" instead of "imaging platform").

Reviewers' comments:

Reviewer #1:

Manuscript Summary:

The authors present here a pipeline for image acquisition and subsequent analysis of Q40-YFP aggregates in the nematode C.elegans. They nicely summarise and refer to all publicly available resources to provide a step-wise analysis. My concern is however, that this described pipeline works only for well-defined foci in large cells such as Q40-YFP in muscles and is therefore of very limited use for analysis of e.g. neurons and other type of aggregation-prone proteins. See specific comments below.

Major Concerns:

1. A major limitation of that protocol is the nature of the aggregates. PolyQ aggregates can be easily identified by imaging software such as Cell Profiler as individual signals. To demonstrate that this protocol (as the authors claim) is useful for other aggregation-prone proteins as well they should demonstrate it on Abeta, TDP43, FUS etc aggregates. Or simply eliminate these statements. The same is true for the cell type. It all works well in large cells such as muscles and might also work in intestinal cells. But, neurodegenerative diseases affect - well neurons. They are much smaller in size and this imaging approach might not work.

We agree with the reviewer and eliminated these statements throughout the manuscript:

- To better reflect that protein aggregation can occur in various tissues we removed "many of which are neurodegenerative" from the introduction (line 51).
- We removed the last paragraph of the representative results section, which speculated about future applications (see below).
- In the discussion, we included "The fluorescence microscopy step can also be adjusted, for example using higher magnifications to monitor protein aggregation in neurons" (line 382-383).
- In the discussion, we rephrased the last sentence to "Whereas the method was demonstrated for polyQ aggregation in the *C. elegans* muscle tissue, **future applications** of the protocol may include other proteins and tissues, as well as studying the effects of proteostasis factors and small molecules" (line 401-403).

We also clarified that the data fitting in Amylofit is based on the availability of strains with multiple protein concentrations, which are availabe in the case of Q40-YFP in the muscle cells but have not yet been generated for other proteins and tissues: "NOTE: This step can only be performed when data for multiple protein concentrations are available. For Q40-YFP, a set of four strains with different levels of overexpression in the body wall muscle cells has been created previously. In other cases, novel strains should be generated using plasmid micro-injection and genomic integration." (Step 6, line 265-268)

2. Q40-YFP foci are well characterised aggregates, yet this imaging approach fails to discriminate between simple assemblies of still soluble proteins and aggregated insoluble proteins as will be the case for any other amyloid proteins or polyQ proteins with flanking regions that show a more heterogeneous as well as dynamic aggregation pattern. This was not addressed in this protocol.

We agree with the reviewer that we have only demonstrated the detection of Q40-YFP aggregates with our protocol, and cannot draw conclusions for other proteins or aggregation pathways. We have adjusted the manuscript as outlined in our response to major point 1 above.

We also adjusted the headers of steps 5 and 6 in the protocol to specify that the method is based on counting the numbers of inclusions, without considering different aggregation states:
"5. Automated inclusion counting using CellProfiler" (Line 215)
"6. Global fitting of inclusion count data using AmyloFit" (Line 263)

3. It would be helpful to comment on challenges throughout the protocol. NaN3 is a harsh method to immobilise nematodes. Would a polymer such as provided by Nemagel or anaesthetic such as levamisol work as well?

The JoVE format does not allow us to include too many challenges and alternative methods in the protocol itself. However, we included these suggestions in the revised discussion: "Sodium azide is a relatively harsh anesthetic, which could be replaced by physical immobilization with hydrogels or beads" (line 389-390).

4. The figures are of very low resolution. So low that one cannot even read axis labelling.

We regret that the resolution of figures 1 and 3 was greatly reduced in the submission process. The figures will be submitted as pdf (instead of jpeg) together with the revised version of the manuscript to solve this issue.

5. In the discussion section, different methods of synchronisation of C.elegans were compared. However, the auxin-inducible system by employing the strain PX627 was missed and should be included.

The discussion has been rewritten to be more concise, according to the editor's instructions (editor point 10). We included only the most common methods for synchronisation that could be applied as an alternative for the strains that we used.

6. Throughout the protocol it is stressed that this procedure can be used to screen genes or small molecules. Yet no example is provided and the reason might be the very labor-intensive step of transferring individual animals into the 384 wells. The authors should demonstrate the feasibility or eliminate statements on high-throughput analyses.

The reviewer is correct that we do not provide an example of screening for drugs or small molecules. Indeed the throughput of the current methods is a limitation, as included in the revised discussion: "The throughput of the technique is currently limited by the need for manual picking of the animals into the 384-well plate. This can potentially be remedied by the use of micro-fluidic devices." (line 387-388).

We rephrased the last sentence of the abstract to: "The method here displayed ***may*** prove useful to assess the effects of proteostasis factors and potential therapeutics for protein aggregation diseases in a living animal in a robust and quantitative manner." (line 45-47)

We also removed "high-throughput" in the introduction (line 80), removed the last paragraph of the representative results section and rephrased the last sentence of the discussion as detailed in the response to major point 1.

Minor Concerns:
The authors should make sure that all gene names as well as C. elegans are italicised.

We apologise that *C. elegans* was not italicised in the reference list, this has been corrected. We are not aware of any gene names in the manuscript.

Line 108: replace "recycled" by "reused"

Adjustment has been made (line 118 in the revised manuscript).

Line 178: "one module at a time" instead of "on module at a time"

Adjustment has been made (line 242 in the revised manuscript).

Reviewer #2:
Manuscript Summary:
The manuscript by Molenkamp et al describes a semi-automated method that allows to monitor inclusion formation of PolyQ proteins expressed in C. elegans. The advantage of the presented pipeline is that it allows to quantify aggregation kinetics , as well as using mathematical modeling that allows to establish biophysical parameters that drive protein aggregation in vivo.

Minor Concerns:
I don't really have any major concerns. The manuscript is well written and the method described in sufficient detail so that anyone should be easily able to follow it. My only suggestion would be to highlight already in the introduction how and why this method is important to quantify aggregation and understand the molecular mechanism of aggregation. The authors mention this very briefly in the last paragraph of the introduction, but this could be expanded a bit more e.g. students who may not be so familiar with the topic.

We appreciate the feedback from the reviewer. For those new to the field, we included in the revised introduction the notion that it is not yet clear how aggregation is linked to toxicity, and that therapeutics for protein aggregation diseases are not yet available: "The misfolding of these polypeptides into amyloid fibrils is associated with toxicity and cell death by mechanisms that are still largely unclear. Elucidating the mechanisms of amyloid formation will be crucial to develop effective therapies that are currently unavailable." (line 54-57)

In the Protocol Section, point 3 (Image acquisition): please mention already here that a confocal microscope can

also be used as an imaging platform if it is equipped with a multi-well plate holder (not every lab or facility has an high-throughput imaging platform). The authors do mention this later on in the discussion, but it is worth mentioning in the method description as well.

We thank the reviewer for this suggestion. Although notes in the protocol should be used sparingly according to the editor's instructions, we have moved this information from the discussion to a note in step 3. "NOTE: This experiment can also be set up on a regular spinning disk confocal microscope with multi-well plate holder. A camera with a large field-of-view is however beneficial to limit the number of tiles to be imaged to span the entire well." (Line 145-147)

Reviewer #3:
Summary:
This manuscript demonstrates a method for quantifying protein aggregation kinetics in C. elegans in vivo in a semi-automated manner using CellProfiler and further fitting into mathematical model using AmyloFit.

Overall analysis:
The method described in this paper warrants consideration for publication. The authors show an innovative method to quantify protein aggregation kinetics. This method is confocal-microscopy-centered, while the reagents/software are easy to obtain. However, there are several areas that need to be addressed. First, details of the method are either lacking or are difficult to locate, leaving the reader with a superficial knowledge but lacking critical information to easily implement the method (specifics listed below). Second, the accumulation of aggregates is usually, but not always, associated with declining function of the proteome. Sequestration is a known mechanism to safeguard the proteome by removing toxic species from direct interaction. Typically, in addition to the direct qualification of fluorescent foci, a secondary assay is included to measure muscular function. For instance, in many cases an age-associated paralysis assay or in rarer cases an assessment of overall levels of insoluble proteins is included to confirm that increased foci accumulation is a sign of proteome collapse. The authors do not need to include such a method, as published examples are available (including JoVE). But the authors need to discuss this limitation in their assay and reference secondary approaches to address it.

We appreciate the reviewer's analysis of both the strengths and limitations of the protocol. We have addressed the detailed comments in the revised manuscript as outlined below.

Major concerns:
1. The "high-throughput imaging platform" mentioned by the authors in the abstract and introduction is needlessly vague. The authors should describe the use of confocal and the 384 platform in some detail within the introduction.

Unfortunately the JoVE format does not allow us to mention the specifics of the brand or model of the equipment. However, we agree with the reviewer that the term "high-throughput imaging platform" is rather vague and have replaced this by "high-throughput confocal microscope" throughout the text.

2. Step 3 requires a confocal microscope with a 384 well adaptor, which is not a standard piece of laboratory equipment. What is the platform adaptor they are using? This will limit utility in some institutions. Furthermore, it is unclear whether all of the mentioned settings are standard options across confocal setups.

Our protocol is based on the instrument listed in the Table of Materials, which is dedicated to image multiwell plates. Unfortunately the settings as stated in the protocol are indeed specific to this instrument and will need to be adjusted by users who will perform our protocol with different equipment.

3. For step 4, it would be useful to include a supplemental figure that shows step by step screenshots of how to use ImageJ to stich tiled images together.

We appreciate this suggestion and have included a new figure (Figure 2) showing the stitching procedure.

4. What platforms/operating systems can run CellProfiler (step 5)? This could also be a limitation in utility.

CellProfiler is compatible with MacOS and Windows. As such, we do not expect this to be a limitation.

5. What is "post-processing?" Step 5.8 (line 186)? This needs to be defined.

This step (5.9 in the revised version) has been rewritten to improve the clarity and move non-actionable items into the note (see editor point 4): "5.9 Open the output folder to view the output files. NOTE: The number of inclusions per worm can be found in the file named "ExpandedWormObjects". Additional information about the input images can be found in the file named "Image". An image of the worms and inclusion outlines is saved for

manual inspection. Additional output can be selected in the ExportToSpreadsheet module in the pipeline." (Line 254-260)

6. Line 207: "enter the equation to fit the data" doesn't make sense until the reader gets to the results section and is jarring to the reader. Is the equation always the same? Are there examples of specific experimental setups where one equation would be more appropriate than another? If true, then the authors should provide a supplemental table to define conditions where a specific equation is needed. For all possibilities the authors should provide an appropriate equation or give additional guidance for how one would determine the correct equation and how to enter it. Clarification is needed here.

The reviewer is correct that specific instructions were missing here (see editor point 4). We have included the equation that should be used to fit the data for Q40-YFP in the muscle cells in Step 6.5: "Select Custom in the model panel, enter Ncells*(1-exp(-Kcell*m**(n)*(t-1))) in the equation box and click Load model." (Line 288-289)

We furthermore revised Figure 4B to show the equation.

7. Line 210: the authors should either provide models in a supplemental table and not refer the reader to a reference, or rephrase this text to indicate that independent (and not cooperative) models are appropriate for fitting nucleation within body wall muscle. The purpose or rationale for examining "cooperative nucleation" is unclear. The manuscript first mentions cooperative nucleation in the protocol (line 210) without providing a brief description or distinguishing it from "independent nucleation." Interpretation of representative results that the "cooperative aggregation kinetics…does not match the kinetics of Q40-YFP inclusion formation" (lines 240-241) is not discussed.

We agree with the reviewer that the use of the cooperative model is confusing and we have removed it from the protocol and the representative results in the revised version of the manuscript. However, we would like to point out that other models may be required to fit other types of aggregation data. Therefore we have included the following in the revised discussion: "The analysis in Amylofit here presented is based on an aggregation mechanism consisting of independent nucleation events in individual cells. In cases where this model does not fit, the user should consider an alternative such as the cooperative aggregation model developed previously." (Line 392-395)

8. In the representative results, the authors reported the aggregation kinetics of Q40 as "a nucleation rate constant of 2.7 x 10-12M-0.94s-1, corresponding to a nucleation rate of 0.01 molecules h-1 per cell at an intracellular protein concentration of 1mM, and a reaction order of 1.94" (lines 235-237). The authors do not provide any information about the known aggregation kinetics of Q40 and how the nucleation rate constant from their mathematical model is compared to that data. The authors do not mention the number of trials and how the nucleation rate differs between each biological replicate. This difference is an important factor should this method become a more standardized protein aggregation quantifying protocol.

The reviewer raises a valid question regarding the reproducibility of the method. In the revised version, we have included a comparison between two independent datasets (Table 1), demonstrating the robustness of the method.

We added to the text: "Two independent biological replicates led to closely corresponding values for the nucleation rate and reaction order which are in agreement with a previous study using a similar protocol (Table 1)." (Line 333-335)

We also added to the legend of the revised Figure 4: "The data are representative of two independent biological replicates." (Line 357)

9. The authors mention "motility defects" (line 73) in the introduction but do not discuss it afterwards. Motility is an important readout for toxicity in polyQ aggregation assays, and the authors do not discuss how they will put the nucleation rate constant from their mathematical model into the context of proteotoxicity.

The protocol does not address motility and "which correlates with motility defects" has been removed from this sentence in the introduction (line 74).

Minor concerns:
1. Line 73: The authors should reference manuscripts that use similar transgenic approaches within intestinal cells (currently missing).

We have added "and the intestine" with the appropriate references (line 75).

2. Step 1.4: how many animals are typically transferred?

We have included this information in Step 1.4: “Transfer ca. 40 animals per strain times the number of points to be imaged, to compensate for animals that die or are lost during transfer (see Step 2).” (line 107-108).

3. Step 2.3: "after transferring them there when necessary" is awkwardly written.

This sentence has been rephrased and moved to the note: “The worms must be placed outside the bacterial lawn before picking them into the well.” (line 130-131).

4. Step 2.5: the authors need to give an approximation of a typical number of time points that will be needed for control conditions.

This information has been included in the representative results section: “From day 1 up to day 10 of adulthood” (line 321) and is also shown in Figure 4C.

5. Step 4.3 There is no mention in earlier steps that it is important to note the "type" of tile, nor the order in which images are collected.

The order by which the tiles were collected was left to the default setting of the instrument in Step 3. In response to major point 3, we added the new Figure 2 and associated text which further clarify this step of the protocol: “The images of the wells were acquired as 6 tiles, which were stitched together using a plugin in ImageJ (Figure 2).” (Line 323-324)

6. Step "6.7" (line 184) should be 5.7.

Corrected in the revised version.

7. Step "6.8" (line 185) should be 5.8.

Corrected in the revised version.

8. No mention of number of biological or technical replications.

As responded to major point 8, we included this information in the revised version.

9. The bottom right three panels in Figure 2 lacks specification in the figure legend. What does each panel stand for? What do the arrows mean?

We apologise for this omission in the legend of this figure (Figure 3 in the revised version). To clarify the meaning of the panels and arrows, we have labelled the panels and revised the legend as follows: “Figure 3. Schematic of the CellProfiler pipeline to quantify inclusions numbers. A-C) The brightfield image (A) is used to identify the worms (B, close-up in C). D-G) The fluorescence image (D, close-up in E) is used to identify the inclusions (F). The worms and inclusions are related to provide the number of inclusions for each worm in the well (G). The images shown are of Q40 line A animals at day 3 of adulthood.” (Line 348-352)

10. In Figure 3B, the models for independent nucleation and cooperativity is not mentioned in the legend.

We removed the cooperative model from the protocol and from the figure (see major point 7), and included the equation for independent nucleation in the new Figure 4B.

11. Figure 3 in general is too blurry to see the details.

As responded to reviewer 1, major point 4, we regret that the quality of figures 1 and 3 was lost during the submission process. We revised figure 3 (now Figure 4) and will submit it as a pdf file.

12. In the summary section, it seems like the protocol is looking at the same animals at different timepoints (line 23-24), which does not match the protocol section in which different animals from the same parents are imaged at different timepoints.

We understand that the sentence in the summary could be interpreted as such, and rephrased this into “Animals from an age-synchronized population are imaged at different timepoints” (line 23-24).

13. Step 1.3 (lines 98-100)- How will the animals grow to adulthood on NGM plates? Won't they arrest at L1 due to lack of food?

The NGM plates are seeded, as inserted in step 12 in the revised version (line 96).

14. The discussion section does not mention situations other than body wall muscle cells. How is this protocol

applicable to aggregation in other tissues like neurons and the intestine? For example, in the neurons, how will a higher magnification and smaller aggregate sizes affect data collecting and the accuracy of the programs?

Indeed the small size of the neurons presents a challenge for the current method. As outlined in the revised discussion, the sample preparation and image acquisition would need to be adjusted, but the data analysis methods will still be applicable: “The fluorescence microscopy step can also be adjusted, for example using higher magnifications to monitor protein aggregation in neurons. (…) The CellProfiler pipeline can still be used in these cases, but the settings (pixel size and intensity threshold to recognize worms and inclusions) will need to be adjusted by the user.” (Line 382-387).